PROCEEDINGS OF SCIENCE

# Probing Axion–Nucleon Interactions with Water Cherenkov Experiments

**Diego Guadagnoli**[a,*]

[a] *LAPTh, Université Savoie Mont-Blanc et CNRS, Annecy, France*

*E-mail:* diego.guadagnoli@lapth.cnrs.fr

We discuss the prospects of using large water Cherenkov experiments, such as Hyper-Kamiokande, to probe two fundamental interactions of the QCD axion: the couplings to nucleons. Starting from the general axion-nucleon interaction in a chiral effective field theory framework, we consider axion emission from nearby core-collapse supernovae and their subsequent absorption in water through processes such as $a + N \to N + \gamma$ and $a + N \to N + \pi^0$. The resulting Cherenkov light spectra can generally be separated from the standard neutrino signal. We outline the theoretical setup, the main observables, and the parametric dependence of the expected event rates on the axion couplings and on the supernova distance. The material presented here is based on Ref. [1].

Preprint: LAPTH-Conf-050/25

*The European Physical Society Conference on High Energy Physics (EPS-HEP2025)*
*7-11 July 2025*
*Marseille, France*

*Speaker



https://pos.sissa.it/

PoS(EPS-HEP2025)182

## 1. Introduction

In this note we outline the possibility of using water Cherenkov experiments, such as Hyper-Kamiokande (HK), to probe two fundamental interactions of the QCD axion, namely the axion–nucleon interactions. This talk is based on Ref. [1].

Water Cherenkov experiments are designed to detect neutrino fluxes from astrophysical sources. Neutrinos are well known to play a crucial role in the cooling of such sources, for instance in core-collapse supernovae (SNe). The same experimental design can, however, also be used to search for fluxes of *exotic coolers*, such as axions, emitted from the same sources. As a baseline study of Cherenkov signals from core-collapse SNe, we refer to Ref. [2].

In what follows we consider the most general axion–nucleon Lagrangian, which serves as a reference case, and investigate how it could be probed through axion absorption in water Cherenkov detectors.

## 2. Strategy and Theoretical Framework

### 2.1 General approach

Our overall strategy can be summarized as follows:

- We consider QCD axions emitted by *nearby* SNe. The significance of "nearby" in this context will be clarified later and is essentially set by detectability thresholds in HK-like detectors.
- These axions are then absorbed on Earth through processes such as

  $$a + N \to N + \gamma, \qquad a + N \to N + \pi^0,$$

  where $N$ denotes a nucleon. Both $\gamma$ and $\pi^0$ are *Cherenkov partons*, i.e. particles that initiate Cherenkov cascades in water.
- The key theoretical ingredients are:
  - the axion emissivity in the SN core (the emitting body),
  - the axion absorption spectra in the detector.

  Both quantities are computed within a consistent effective field theory (EFT), namely Chiral Perturbation Theory (ChPT) extended to include the axion.

### 2.2 Chiral Perturbation Theory and hadronic degrees of freedom

Given the hadronization scale $\Lambda_{\text{QCD}} \sim 1$ GeV, we know that well above this scale strong interactions involve quarks and gluons, while well below this scale it is more convenient to work in terms of hadronic degrees of freedom.

As far as the light-meson octet is concerned, the hadronic Lagrangian $\mathcal{L}_{\text{hadrons}}$ is essentially fixed by the global chiral symmetries of QCD. This gives rise to Chiral Perturbation Theory (ChPT). The crucial advantage of ChPT is that it is a well-defined EFT: observables are calculable with a controlled power counting, with a small expansion parameter schematically given by the ratio $p_\pi / f_\pi$, where $p_\pi$ is a typical pion momentum and $f_\pi$ is the pion decay constant.



PoS(EPS-HEP2025)182

### 2.3 Including the axion in ChPT

The QCD axion has the same quantum numbers as neutral pseudo-scalar mesons such as the $\pi^0$ and the $\eta$. Therefore, ChPT can naturally be extended to include the axion as an additional pseudo-scalar field [3].

In this construction, all the interactions of the axion with an arbitrary number of mesons, and with two baryons and an arbitrary number of mesons are fixed by the global symmetries that define the Lagrangian. All these interactions are ultimately fixed by the fundamental UV interaction, namely the axion–quark coupling, of the schematic form

$$\mathcal{L}_{aqq} \sim \frac{\partial_\mu a}{f_a} \Big( \bar{q} \gamma^\mu P_L k_L q_L + \bar{q} \gamma^\mu P_R k_R q_R \Big),$$

where $f_a$ is the axion decay constant and $k_{L,R}$ are 3-by-3 coupling matrices to $q$, the triplet of light quarks $(u, d, s)^T$.

At the hadronic level, the axion Lagrangian involves the usual chiral meson field $U$ and the baryon field $B$, and includes in particular axion–two-nucleon terms. These take the derivative form

$$\mathcal{L}_{aNN} = \frac{\partial_\mu a}{2 f_a} \sum_{N=p,n} C_{aNN} \, \bar{N} \gamma^\mu \gamma_5 N,$$

with $C_{aNN}$ a calculable function of the underlying axial couplings between the axion and the $u$ and $d$ quarks.

## 3. Modeling the Axion–Nucleon Couplings

The couplings $C_{aNN}$ can be modeled in several ways. We consider three cases of interest:

1. **KSVZ / DFSZ models:** in these benchmark UV-complete models, $C_{aNN}$ are fixed (up to model parameters such as $\tan\beta$ in DFSZ) by the model construction.
2. **Agnostic scenario:** here $C_{aNN}$ are treated as free parameters constrained only by data. Specifically, we impose:
    - *Neutron-star (NS) cooling*, which bounds the axion contribution to NS energy loss, thereby limiting the size of $C_{aNN}$;
    - *Supernova (SN) cooling*, implemented through the Raffelt bound, which requires that the luminosity emitted in axions not exceed the neutrino luminosity, $L_a \lesssim L_\nu$, as inferred from SN1987A [4, 5].

In summary, in the agnostic scenario the allowed region in the $(C_{app}, C_{ann})$ plane is carved out by NS and SN cooling constraints, and the KSVZ/DFSZ models are contained as specific points or lines within this region.

## 4. Axion Detection in Water Cherenkov Detectors

### 4.1 Basic processes and Cherenkov partons

In the core-collapse picture, a SN produces an overdense proto–neutron star that results in a neutrino burst. An important question is whether this burst is accompanied by a burst of *other* coolers, such as axions.

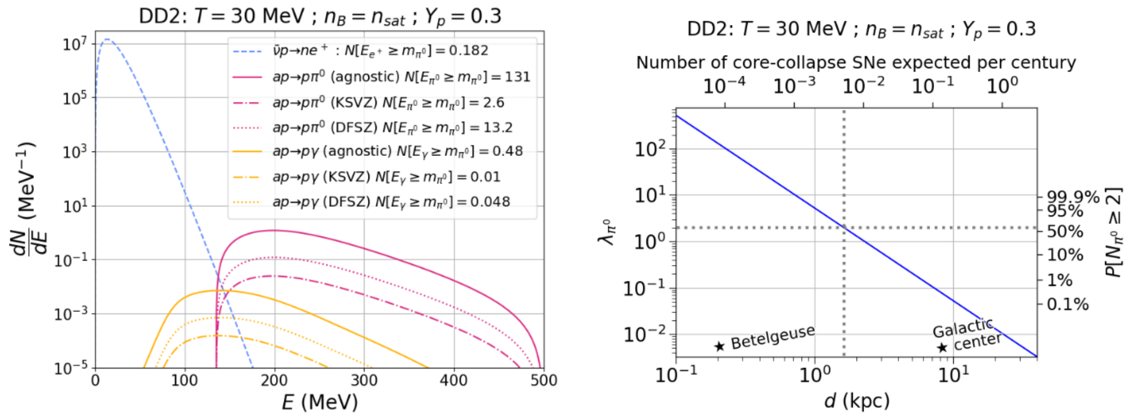


**Figure 1:** (Left) Neutrino- vs. axion-induced Cherenkov spectra for $T = 30$ MeV and the DD2 EOS, assuming $d = 0.2$ kpc; the $\pi^0$ channel is seen to dominate (purple) over photons (yellow), and to peak at higher energies than the neutrino spectrum (blue). (Right) Axion-induced $\pi^0$ event rates $\propto 1/d^2$ versus the SN distance, with detectability threshold at $\geq 2$ events determining the critical radius (dashed lines) for observable axion bursts.

The fluxes of these coolers — neutrinos and a possible axion component — are potentially detectable on Earth through processes of the form

$$\alpha + N \longrightarrow N' + X, \tag{1}$$

where $\alpha$ is the cooler species (either $\nu$ or $a$), $N$ and $N'$ are nucleons, and $X$ is a Cherenkov parton (e.g. $e^{\pm}$, $\gamma$, $\pi^0$) initiating a Cherenkov cascade. The corresponding cross sections are denoted $\sigma_{\alpha X}$.

### 4.2 Number spectra

We aim to compute the number spectrum of a given Cherenkov parton $X$ in terms of the number spectrum of the cooler $\alpha = \nu, a$. The relation is schematically

$$\frac{dN_X^{(\alpha)}(E_X)}{dE_X} = \frac{N_t}{4\pi d^2} \int dE_\alpha \, \frac{d\sigma_{\alpha X}(E_\alpha, E_X)}{dE_X} \, \frac{dN_\alpha(E_\alpha)}{dE_\alpha}, \tag{2}$$

where $N_t$ is the number of detector targets, $d$ is the SN-to-Earth distance, $d\sigma_{\alpha X}/dE_X$ is the differential cross section for the process Eq. (1), and $dN_\alpha/dE_\alpha$ is the number spectrum of the cooler at the source. This integral scales linearly with $N_t$ and quadratically with the inverse distance, $1/d^2$.

## 5. Qualitative Features of the Spectra

### 5.1 Cherenkov spectra and model dependence

The Cherenkov parton spectrum can be visualized for different SN core temperatures $T$. We provide an example in Fig. 1 (left), taken from [1]. The figure shows in blue the $e^+$ spectrum from the neutrino process, in red the $\pi^0$ spectrum from $ap \to p\pi^0$, in yellow the $\gamma$ spectrum from $ap \to p\gamma$. Each of these spectra can be shown for the different model assumptions (KSVZ, DFSZ, agnostic) introduced earlier.

The main take-home messages from such spectra are:

- Cherenkov-light spectra induced by $\nu$ and by $a$ peak at well separated energies.
- The peak from the $\pi^0$ channel is much more promising than that from the $\gamma$ channel, both in terms of separation from the neutrino-induced spectrum and in terms of peak height.

### 5.2 Detector simulations

We also studied the spectrum using a realistic HK setup to estimate the efficiency on the $\pi^0$ signal, keeping in mind that at energies above roughly 140 MeV the signal is essentially background-free.

The main spectral features survive detector effects, as expected: the separation between the neutrino and axion channels is preserved and the relative importance of the $\pi^0$ channel remains dominant.

## 6. Event Rates and Coupling Dependence

### 6.1 Dependence on $C_{app}$ and $C_{ann}$

It is interesting to study how the expected number of $\pi^0$ events due to axions depends on the assumed values of the axion–proton and axion–neutron couplings. Denote the expected number of events in an energy range $R$ by $\lambda(C_{app}, C_{ann}; R)$, which plays the role of the Poisson parameter. One can then study the number of expected events as a joint function of $(C_{ann}, C_{app})$, for different values of $\lambda$. The cooling constraints typically imply that the number of events does not exceed a few $\times 10^2$ for such a nearby SN. Conversely, for a SN explosion at the Galactic center ($d \approx 8$ kpc), demanding, $\lambda \geq 2$ events (as a detectability threshold) selects larger values of $C_{app}$ and $C_{ann}$.

### 6.2 Temperature dependence

One can also study how the previous picture changes with SN core temperature $T$. The $T$ dependence is by far the most pronounced, we note that moving from 30 to 40 MeV causes the expected number of events to change by nearly an order of magnitude.[1] For example, the KSVZ point yields about 5 events at $T = 30$ MeV and approximately 50 events at $T = 40$ MeV. In conservative estimates, one may therefore focus on predictions at $T = 30$ MeV.

## 7. Distance Scaling and Galactic Rates

A final question of interest is how the number of events relates to the number of SN candidates.

As noted above, the number of axion-absorption events scales as $N_{\text{events}} \propto 1/d^2$, where $d$ is the SN-to-Earth distance. The larger the distance, the smaller the number of events, but the larger the number of SN candidates per unit time (i.e. the shorter the waiting time until the next SN explosion somewhere in the Galaxy).

Quantitatively, for a given SN model and $T$ (e.g. $T = 30$ MeV) one can plot the expected number of $\pi^0$ Cherenkov events (due to axions) as a function of $d$. An example is shown in Fig. 1 (right). On the same plot, one can map $d$ to the expected number of CC SNe per century within that radius.

[1]This can be understood from the emissivity dependence: $Q_a \approx T^{7.5}$ multiplied by a factor with non-trivial $T$ dependence. If we neglect this factor, we would thus expect the temperature increase to yield approximately 8.7 times more events.

Over the full Galaxy, one expects $O(1)$ CC SN per century. Requiring an expected number of axion-induced events of at least 2 (our detectability threshold) typically constrains $d \lesssim 2$ kpc. This corresponds to $O(10^{-2})$ or fewer SN explosions per century that are both sufficiently close and produce a detectable axion burst.

## 8. Conclusions and Outlook

In conclusion:

- While HK can detect neutrino bursts from distances up to several Mpc, much smaller distances, of order $d \lesssim 2$ kpc, are required to *also* detect an axion burst.
- Such an axion burst can be detected via axion absorption in

$$a + p \to p + \gamma \quad \text{or} \quad a + N \to N + \pi^0,$$

  with the second process being significantly more promising due to its higher peak and higher characteristic energy.
- Axion signals are generally small in the minimal modeling because we restrict to axion absorption by the protons that constitute the hydrogen in water.

Improving the modeling of axion absorption in water is essential to uncover possible order-of-magnitude enhancements. On the theory side, this includes accounting for absorption on neutrons and contributions from oxygen nuclei. On the experimental side, it requires larger detector volumes (increasing target numbers) and improved $\pi^0$ reconstruction at $O(100\text{ MeV})$ energies.

**Acknowledgments—** I would like to thank my co-authors M. Cavan-Piton, A. Iohner, P. Fernández-Menéndez and L. Vittorio for an enjoyable collaboration on Ref. [1], and the conveners of track 03 for the stimulating sessions. This work has received funding from the French ANR under contracts ANR-19-CE31-0016 ("GammaRare") and ANR-23-CE31-0018 ("InvISYble"), which is gratefully acknowledged.

## References

[1] M. Cavan-Piton, D. Guadagnoli, A. Iohner, P. Fernandez-Menendez and L. Vittorio, *Probing the general axion-nucleon interaction in water Cherenkov experiments*, *JHEP* **07** (2025) 070, [2503.17490].

[2] G. Lucente, L. Mastrototaro, P. Carenza, L. Di Luzio, M. Giannotti and A. Mirizzi, *Axion signatures from supernova explosions through the nucleon electric-dipole portal*, *Phys. Rev. D* **105** (2022) 123020, [2203.15812].

[3] H. Georgi, D. B. Kaplan and L. Randall, *Manifesting the Invisible Axion at Low-energies*, *Phys. Lett. B* **169** (1986) 73–78.

[4] G. G. Raffelt, *Astrophysical methods to constrain axions and other novel particle phenomena*, *Phys. Rept.* **198** (1990) 1–113.

[5] A. Caputo and G. Raffelt, *Astrophysical Axion Bounds: The 2024 Edition*, *PoS* **COSMICWISPers** (2024) 041, [2401.13728].